

Near-Field Modification of Interference Components in Surface Plasmon Resonance

Robert P. Schumann and Stephen Gregory
Department of Physics, Oregon Center for Optics
and
Materials Science Institute
University of Oregon
Eugene, OR 97403-1274

In an attenuated total reflection (ATR) geometry, energy extracted from an incident light beam by surface plasmon polariton (SPP) creation is implicitly considered to dissipate as heat. However, we show that a sharpened tip interacting with the SPP evanescent field can redirect some of the energy before such dissipation occurs. This behavior is examined with simple computer simulations and an analogy is drawn between it and a modified Mach-Zehnder interferometer. We also discuss "interaction-free" measurements with our set-up.

PACS numbers: 42.25.Gy, 42.50.St, 73.20.Mf

For a metal film in an ATR geometry, a minimum in the reflected light intensity at a specific angle is usually viewed as a signature of surface plasmon resonance (SPR). While this no doubt is the case, all that can *directly* be concluded is that there is some energy "missing" from the specular beam. As momentum conservation prevents light transmission beyond the film (if it is smooth) one infers that the missing energy corresponding to the minimum is deposited in the film as heat, and this can indeed be readily detected. [1]

On the other hand, the standard analysis of the ATR geometry [2] is not specifically concerned with energy, but instead considers the interference of light reflected from the front and back surfaces of the film and reproduces the experimentally-observed minimum. As with all interference phenomena, the existence of a minimum in one interference outcome implies a maximum in a complementary outcome. Reconciling the energy and interference pictures indicates that the missing energy must be carried into the complementary outcome as SPPs and eventually converts to heat. However, this sequence is not necessarily inevitable, because one may imagine intercepting some of this energy and redirecting it - essentially changing the destiny of the SPPs. To realize this situation we use the tip of an apertureless near-field scanning optical microscope (A-NSOM) to redirect some SPP energy and examine the effect of this on the specular minimum. When specifically studying SPPs this A-NSOM variant is referred to as a scanning plasmon near-field microscope (SPNM). [3, 4]

In the Kretschmann-Raether (K-R) [2, 5] ATR geometry light is incident through a dielectric prism, on the hypotenuse of which a thin metal film is deposited. (See Fig. 1.) Our SPNM employs a hemispherical glass prism and maintains either a vacuum or inert gas atmosphere ("ambient") over the metal film surface, allowing us to take advantage of the optimum performance of silver as a material for studying SPPs. The scanning probe is tungsten, which does not itself support SPP modes and

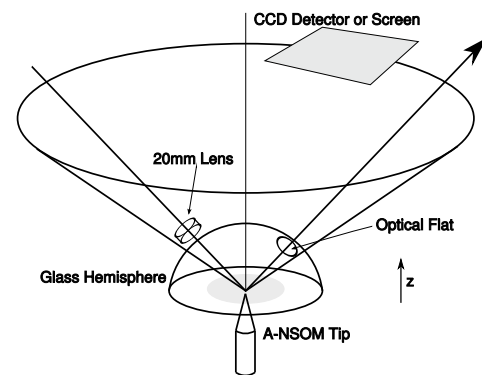


FIG. 1: Experimental arrangement for observing specular reflection and SPP ring

can be etched to a very sharp tip. Incident light with a wavelength of 632.8nm is focused on the silver film with a 20mm lens, in combination with the 25.4mm radius surface of the prism. The calculated beam waist is approximately $3\mu\text{m}$, giving an approximately $5\mu\text{m} \times 3\mu\text{m}$ elliptical spot at the metal film.

It is important that our incident beam is focused, but initially let us consider the reflection of a plane wave in a dielectric-metal-dielectric structure. Solution of the Fresnel Equations for this multilayer system gives the following expression for the reflectivity:

$$r_{123} = \frac{r_{12} + r_{23} \exp(2ik_{2z}d)}{1 + r_{12}r_{23} \exp(2ik_{2z}d)} \quad (1)$$

The first dielectric (the prism in our case) is medium 1, the metal film is medium 2 and the ambient is medium 3. d is the film thickness and k_{2z} is the component of the wave vector in medium 2 perpendicular to the interfaces. Writing the reflectivity in this form emphasizes that the numerator is the sum of the reflections r_{12} from the glass/metal interface and r_{23} from the metal/ambient interface, the latter being modified by the factor $\exp(2ik_{2z}d)$. As k_{2z} has a large imaginary part,

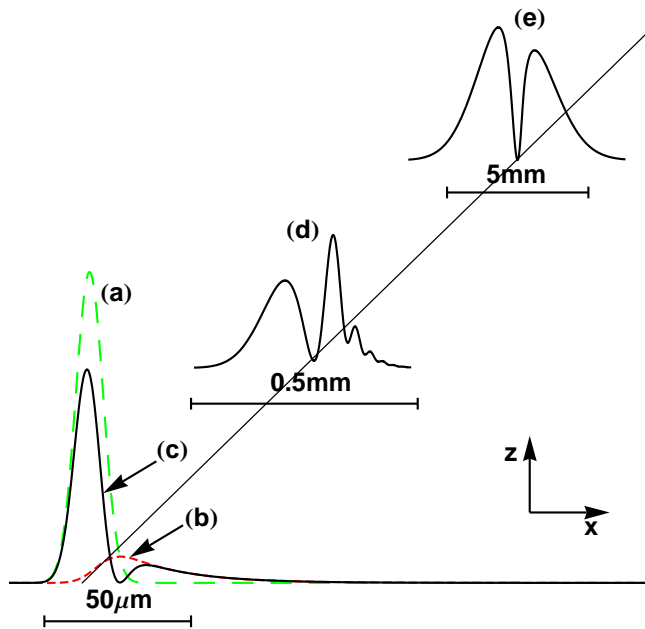


FIG. 2: (Color online) Propagation of the specular beam. Distance is measured from the incident Gaussian center at the 1-2 interface (0mm) along the direction of the SPR far-field minimum. Intensities of: (a) the component reflected from the 1-2 interface, (b) the component reflected from the 2-3 interface and (c) the summed 1-2 and 2-3 interface reflected components, all evaluated at 0mm; (d) the propagating sum at 6.1mm; (e) the propagating sum at 10.1mm. Scale bars indicate increasing width of the beam profile.

this factor decreases exponentially with film thickness. Above the critical angle r_{12} varies only slightly with angle of incidence; r_{23} , on the other hand, is peaked and because it shifts into antiphase with r_{12} at the “resonance angle”, r_{123} displays a minimum at that angle, the depth of which is non-monotonic in d .

In the case of an incident focused Gaussian beam the above approach can be extended by wave-vector decomposition of the incident field [6, 7, 8] and calculation of the reflected fields. Fig. 2 shows spatial profiles of the separate intensities reflected from the 1-2 and 2-3 interfaces as well as the summed beam intensity. As the sum propagates in medium 1 it exhibits oscillations at distances intermediate between the near- and the far-field. Interestingly, however, these are present in the intensity of r_{23} alone. Similar oscillations have been predicted and observed for an ATR apparatus involving two-surface “long-range” surface plasmons. [9, 10]. It is possible, with an appropriate lens, to retain oscillations in the far-field. Since the spherical surface of the prism also has this effect, to obtain a far-field beam free of oscillations we polish a small optical flat into the prism (see Fig. 1) and the expected “notched Gaussian” is then observed.

Although there is no propagating solution for the field in medium 3, there exists a formal solution which de-

cays exponentially in the negative z -direction; i.e. it is evanescent. The x -dependent profile of this solution is identical to that of r_{23} , so its intensity is not shown in Fig. 2. It can, however, be identified with the SPP field propagating and decaying along the interface.

The above treatment is necessary to produce details of the focused Gaussian beam situation, but for much of the following discussion we can refer to the simpler plane-wave expression, Eq. (1). From this we can see that there is a critical thickness d_0 , defined by $r_{23} \exp(2ik_{2z}d) = -r_{12}$ at which the notch in the specular beam reaches maximum area (and zero intensity). Suppose now that, all else remaining the same, r_{23} is somehow reduced to αr_{23} , where $\alpha < 1$. If the film thickness $d < d_0$, the notch area in the specular beam is *increased*, which might seem surprising, if viewed in terms of a “stronger SPR”. However, it is quite consistent with an energetic perspective: The notch is larger because less energy is present in the specular beam, and this accords with any mechanism that reduces r_{23} by dissipation or scattering. On the other hand, if $\alpha < 1$ and $d > d_0$, the notch area is *decreased*. Although more energy is present in the specular beam, more energy also is dissipated or scattered by the mechanism reducing r_{23} . The source of the latter energy can only be SPP energy that otherwise would eventually have been “lost” as heat.

We investigate the cases contrasted above by modifying the r_{23} field with a SPNM tip. In these runs, the tip is moved only in the z -direction. However, we also perform STM and A-NSOM-type scans to judge the quality of our deposited films. If the incident beam is focused to a small spot, the tip can interact with a substantial portion of the SPP field. (It will also interact with the non-resonant components of the evanescent field of the incident beam, but to a much lesser extent, dependent on the film thickness.) The main effect of bringing the tip near the metal surface is to elastically scatter SPPs within the plane of the interface. [3] These can subsequently decay into an expanding hollow cone of radiation [4] that can be detected outside the hemisphere with a CCD camera. The light either impinges directly on the CCD detector or, if the image is too large, onto a translucent screen, which can then be imaged.

Fig 3 is an image of part of the circular conic section (“SPP ring”) and the specular Gaussian beam. Note that the notch is only approximately centered, the exact position within the Gaussian profile depends on the angle of incidence. The ring intensity and notch profile calculated from the appropriate pixel values are plotted in Fig 4 against separation of the tip from the metal surface. Data for a 40nm and 60nm film are shown. At a wavelength of 632.8nm, the critical thickness of a silver film is calculated to be $d_0 \approx 55$ nm. The notch area is calculated as the area between the specular beam profile and a Gaussian fit based on the outer regions of the profile.

For the 40nm film, at large tip-surface separation the

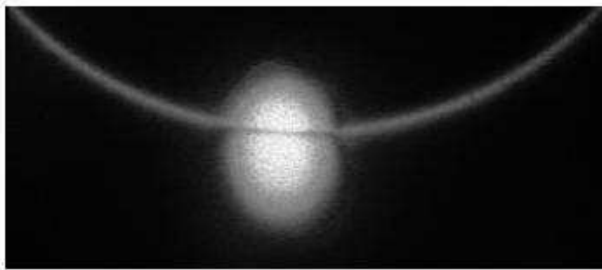


FIG. 3: Specular reflection spot and portion of SPP ring. To show the ring most clearly, the tip is within tunneling distance of the surface.

notch area increases as the tip approaches the surface, but initially the ring intensity does not increase. It is possible that, for large separation, the tip just dissipates energy (as heat in the tip) and does not appreciably scatter SPPs. Modeling this behavior by adding a small imaginary part to the dielectric constant of medium 3 which depends inversely on separation reproduces the observed behavior for r_{123} . At a separation of about 250nm the ring intensity begins to increase, indicating that the tip is elastically scattering SPPs. The notch area now begins to decrease, again in agreement with the expected behavior of r_{123} as $|\alpha r_{23} \exp(2ik_{2z}d)|$ becomes less than $|r_{12}|$. The ring intensity continues to rise and the notch area continues to decrease until the separation reaches about 70nm. Here the notch exhibits a sudden phase and zenith angle shift, the area rising slightly. There is a matching feature in the ring. With smaller separation the ring intensity continues to rise, but the notch area remains fairly constant.

For the 60nm film, the notch area decreases monotonically with decreasing tip-surface separation, but as with the 40nm film and for the same reason, the ring intensity does not increase until about 250nm. (Above this separation the ring intensity actually seems to be non-zero and decreasing slightly, but this is probably an artifact.) With continued decrease of the tip-surface separation, the notch area decreases monotonically. At about 250nm the ring intensity begins increasing rapidly, as with the 40nm film, indicating that elastic SPP scattering is now occurring. At present, we do not understand the significance of the 250nm separation. We note, however, that this same value was obtained in Ref. 4. When the separation reaches about 90nm there are features in both the notch area and ring intensity similar to those for the 40nm film.

The area of the notch for small separation is rather important: In principle, the total energy available for production of either the SPP ring or heat is that which is missing from the specular beam i.e. the notch. If the tip could somehow scatter *all* that notch energy into ring energy then the energy corresponding to the minimum

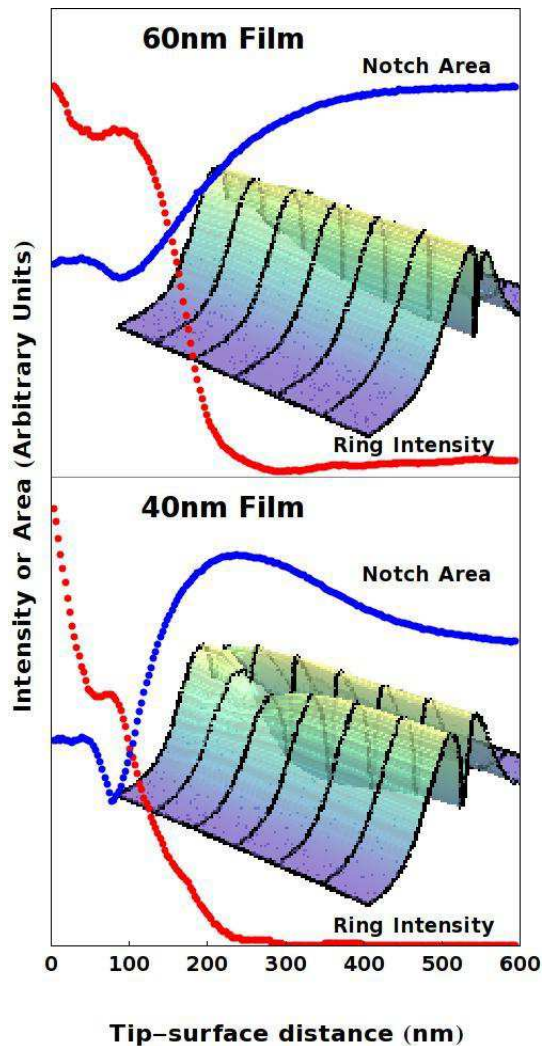


FIG. 4: (Color online) Dependence of the area of the specular notch and the total ring intensity on the tip-surface distance for 40nm and 60nm silver films. Inset surfaces are the profiles of the specular spot as a function of tip-surface distance.

notch area would be equal to that ring energy. In practice, however, scattered SPPs can later decay into heat and the scattering efficiency of the tip depends on the tip shape and distance of the tip “downstream” from the center of the incident beam. Thus, the small-separation notch area is larger than the limiting minimum value. It is interesting that, even after the notch area becomes constant, the overall efficiency of ring light production continues to rise at small separations - quite dramatically in the case of the 40nm film.

We point out that our SPNM experiment is analogous to the modified Mach-Zehnder interferometer shown in Fig. 5a. Absent the extra (dashed) beamsplitter, the lengths of the arms and split fractions are adjusted such that no light reaches detector A. In the SPNM, the partial reflection off the 1-2 (glass-metal) interface and the partial conversion to a propagating SPP wave along the

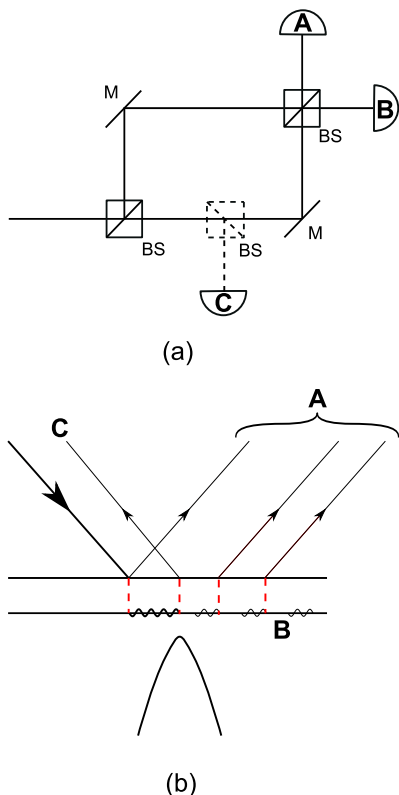


FIG. 5: (Color online) (a) Mach-Zehnder arrangement with extra beam-splitter. A, B and C are light detectors, BS and M denote beam splitters and mirrors respectively. (b) Schematic of the ATR arrangement with movable tip.

2-3 (metal-ambient) interface are analogous to the effect of the first beamsplitter in the Mach-Zehnder interferometer. A difference is that the SPNM produces a light wave and a SPP wave which, in a particle picture, would be viewed as photon-SPP superposition. Subsequently, the reflected wave propagates out to the far field, which we analogize to traversal of the upper arm in the interferometer. The SPP wave, on the other hand travels, in the absence of the tip, an exponentially-distributed distance along the 1-2 interface and tunnels to a wave in the glass which also then propagates out to the far field. The observation of the notch produced by the sum of the two outgoing waves at "A" in the far field is analogous to the observation of no light at detector A in the interferometer, (although the notch is not a perfect null in our experiments). We identify the distributed conversion of the SPPs to heat with the output to detector B in the interferometer.

As already discussed, the presence of the tip (except for the large separation range of the 40nm film) causes an increase in the light detected in the notch while also causing light to be detected in the SPP ring. In the two-dimensional representation of Fig. 5b this is indicated by C, which can actually be anywhere in the ring. In

the same way, the introduction of another beamsplitter into the lower arm of the interferometer causes light to be measured at detector A while also producing light at detector C. We have previously argued that, in our experiment, the presence of the tip redirects some energy that would have dissipated into heat, and which we have labelled "B" in Fig. 5b. Similarly, in the interferometer the introduction of the extra beamsplitter has the effect of decreasing the light measured by detector B. Note that advancing the tip in the SPNM experiment has an interesting advantage over the introduction of a beamsplitter in the interferometer: There is no extra phase shift in the former situation because the tip interacts with an evanescent SPP field, and so the new element does not unbalance the interferometer.

When the input of the SPMN is a greatly attenuated (single-photon) source and we photon count, collecting light with a multimode fiber from the notch minimum, the arrangement is essentially equivalent to that in the Elitzur-Vaidman (EV) "bomb-detector problem" [11] and its experimental realization. [12] In our experiment, the increased rate of photon detection (in principle from zero, which can be approached for a film of thickness d_0), is an "interaction-free measurement" of the presence of the tip. On the other hand, photons detected at C (i.e. in the ring) are essentially equivalent to an explosive detection of the EV bomb and are always anticoincident with those at A. We continue to explore the consequences of this kind of detection for near-field microscopy.

Sponsored by ONR through the Oregon Nanoscience and Microtechnologies Institute.

-
- [1] T. Inagaki, K. Kagami, and E. T. Arakawa, *Phys. Rev. B* **24**, 3644 (1981).
 - [2] H. Raether, *Surface Plasmons on Smooth and Rough Surfaces and on Gratings* (Springer-Verlag, Berlin, 1986).
 - [3] M. Specht, J. D. Pedarnig, W. M. Heckel, and T. W. Hänsch, *Phys. Rev. Lett.* **68**, 476 (1992).
 - [4] Y.-K. Kim, P. M. Lundquist, J. A. Helfrich, J. M. Mikrut, G. K. Wong, P. R. Auvil, and J. B. Ketterson, *Appl. Phys. Lett.* **66**, 3407 (1995).
 - [5] E. Kretschmann, *Z. Phys.* **241**, 313 (1971).
 - [6] W. P. Chen, G. Ritchie, and E. Burstein, *Phys. Rev. Lett.* **37**, 993 (1976).
 - [7] V. Shah and T. Tamir, *J. Opt. Soc. Am.* **73**, 37 (1983).
 - [8] S. L. Chuang, *J. Opt. Soc. Am. A* **3**, 593 (1986).
 - [9] R. V. Andaloro, R. T. Deck, and H. J. Simon, *J. Opt. Soc. Am. B* **22**, 1512 (2005).
 - [10] H. J. Simon, R. V. Andaloro, and R. T. Deck, *Opt. Lett.* **32**, 1590 (2007).
 - [11] A. C. Elitzur and L. Vaidman, *Found. Phys.* **23**, 987 (1993).
 - [12] P. G. Kwiat, H. Weinfurter, T. Herzog, A. Zeilinger, and M. Kasevich, *Phys. Rev. Lett.* **74**, 4763 (1995).